Appl Nanosci (2017) 7:633–643
https://doi.org/10.1007/s13204-017-0597-4

ORIGINAL ARTICLE

# Facile synthesis of microporous $SiO_2$/triangular Ag composite nanostructures for photocatalysis

**Sidhharth Sirohi[1] · Anandpreet Singh[1] · Chakit Dagar[1] · Gajender Saini[2] · Balaram Pani[1] · Ratyakshi Nain[1]**

Received: 2 July 2017 / Accepted: 11 September 2017 / Published online: 25 September 2017


**Abstract** In this article, we present a novel fabrication of microporous $SiO_2$/triangular Ag nanoparticles for dye (methylene blue) adsorption and plasmon-mediated degradation. Microporous $SiO_2$ nanoparticles with pore size <2 nm were synthesized using cetyltrimethylammonium bromide as a structure-directing agent and functionalized with APTMS ((3-aminopropyl) trimethoxysilane) to introduce amine groups. Amine-functionalized microporous silica was used for adsorption of triangular silver (Ag) nanoparticles. The synthesized microporous $SiO_2$ nanostructures were investigated for adsorption of different dyes including methylene blue, congo red, direct green 26 and curcumin crystalline. Amine-functionalized microporous $SiO_2$/triangular Ag nanostructures were used for plasmon-mediated photocatalysis of methylene blue. The experimental results revealed that the large surface area of microporous silica facilitated adsorption of dye. Triangular Ag nanoparticles, due to their better charge carrier generation and enhanced surface plasmon resonance, further enhanced the photocatalysis performance.

**Keywords** Photocatalysis · Microporous $SiO_2$ · Surface plasmon resonance · Composite nanostructures

## Introduction

Dyes are vital chemicals used in several applications such as textiles, food, furniture and paint. However, dumping or accidental discharge of dye-contaminated water into the environment creates considerable environmental and health hazards. Dye, once dissolved in water, becomes stable and hence non-biodegradable. The chemical treatment of dyes is not economically viable. Biological treatment is a better solution but it is quite tedious due to requirement of a large area of land and cumbersome operation (Huang et al. 2011). Use of adsorbents, is a simple and effective way for decontaminating dye pollutants (Ghorai et al. 2014). Adsorption process is influenced by numerous factors including surface area of adsorbent, and extent and type of interaction of dye with the absorbent solids (Wu et al. 1997).

Mesoporous silica due to its large surface area, high hydrothermal stability, and diverse surface functionality, has been explored extensively in biomedical applications, including cell imaging, diagnosis, biosensing, intracellular drug delivery (Argyo et al. 2013; Bharti et al. 2015; Chen 2016; Huang et al. 2014; Sharma et al. 2014; Sharmiladevi et al. 2016; Tang and Cheng 2013; Zhang et al. 2015) and controlled pesticide release (Cao et al. 2016). The morphology and the particle size of mesoporous silica strongly influence the absorption and release of drug/pesticide (Lu et al. 2009). Usually mesoporous silica is synthesized by polycondensation of a silica precursor such as tetraethylorthosilicate (TEOS) or tetramethylorthosilicate (TMOS) in the presence of surfactants which act as structure-

**Electronic supplementary material** The online version of this article (doi:10.1007/s13204-017-0597-4) contains supplementary material, which is available to authorized users.

✉ Balaram Pani
balarampani63@gmail.com

✉ Ratyakshi Nain
ratyakshi@gmail.com

[1] Bhaskaracharya College of Applied Sciences, University of Delhi, Delhi 110075, India

[2] Jawaharlal Nehru University, Delhi 110067, India

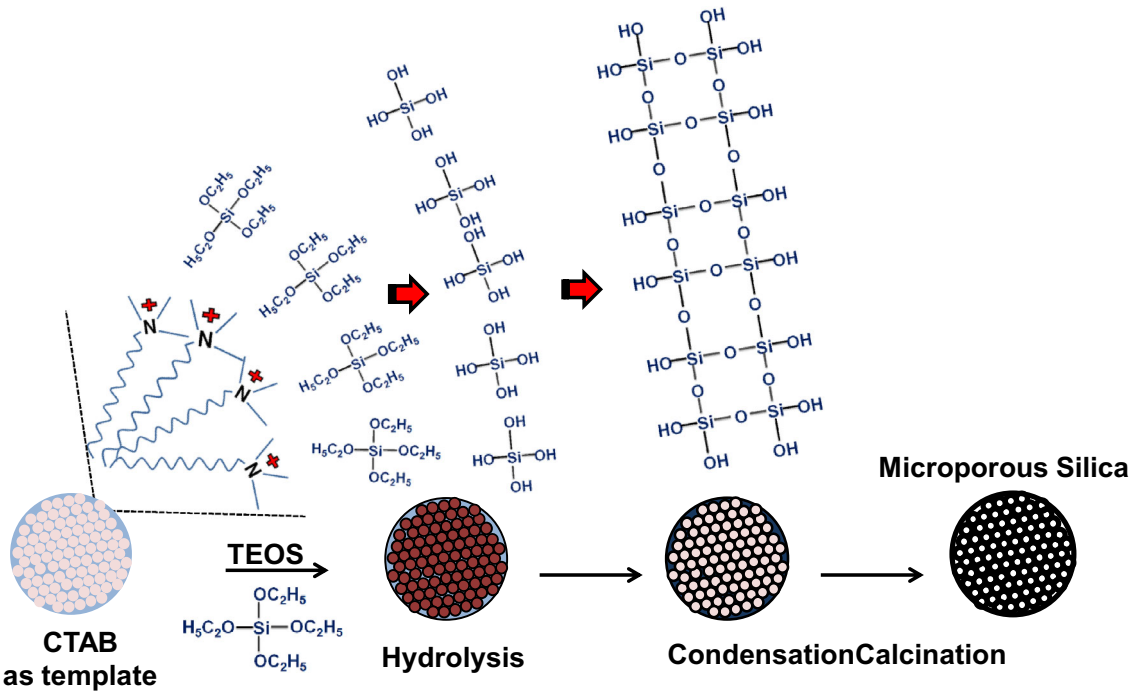


**Scheme 1** Synthesis of microporous silica nanoparticles

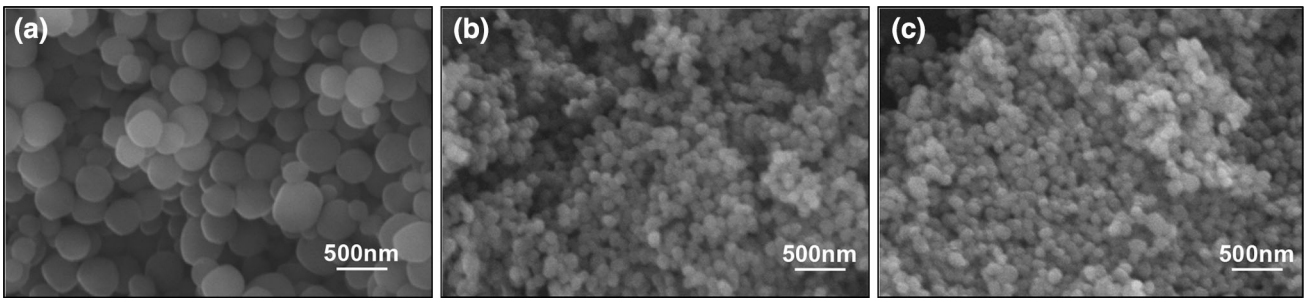


**Fig. 1** Scanning electron micrographs of **a** MS-60, **b** MS-75, and **c** MS-90

directing agents (Giraldo et al. 2007; Wei et al. 2010). Various ionic (cetyltrimethylammonium bromide, CTAB) and non-ionic surfactants (amphiphilic triblock copolymers) can be used for obtaining mesoporous silica with distinctive pore structure and morphology (Wei et al. 2010). The particle size, shape and porosity of particles can be tuned by controlling synthesis parameters, such as pH, reaction time, and temperature. Microporous silica owing to large number of pores with pore size <2 nm, provides ample surface area for materials to get adsorbed on it. The presence of silanol group further ensures better adsorption of dye molecules on its surface (Krysztafkiewicz et al. 2002). Researchers have investigated photocatalytic activity of various nanoparticles (NPs) including $TiO_2$ (Schneider et al. 2014), ZnO (Bandekar et al. 2013; Elmolla and Chaudhuri 2010), $MnO_2$ (Li et al. 2008) and silver (Badr and Mahmoud 2007), etc. The $Ag/SiO_2$ nanostructures with Ag as core material have also been used for sensing (Aslan et al. 2007; Nimrodh Ananth et al. 2011), antibacterial (Alimunnisa et al. 2017) and surface-enhanced Raman scattering (SERS) (Wang et al. 2009) applications. Ag NPs have recently been proposed as a novel photocatalyst for degradation of organic pollutants due to their surface plasmon resonance (SPR) absorption in the visible range. Ag NPs, when excited with photon, energize conduction electrons of 5sp bands and excite them to higher energy states. These excited electrons participate in chemical reactions (Chen et al. 2010). Additionally, holes left in the 5sp bands possess strong oxidizing power and hence act as driving force for photocatalysis. SPR frequency of Ag is a function of its particle size and shape, and triangular silver nanoparticles are reported to have better photocatalytic activity. Non-porous $SiO_2$/Ag core shell nanostructures consisting of yellow Ag NPs prepared using Stober method

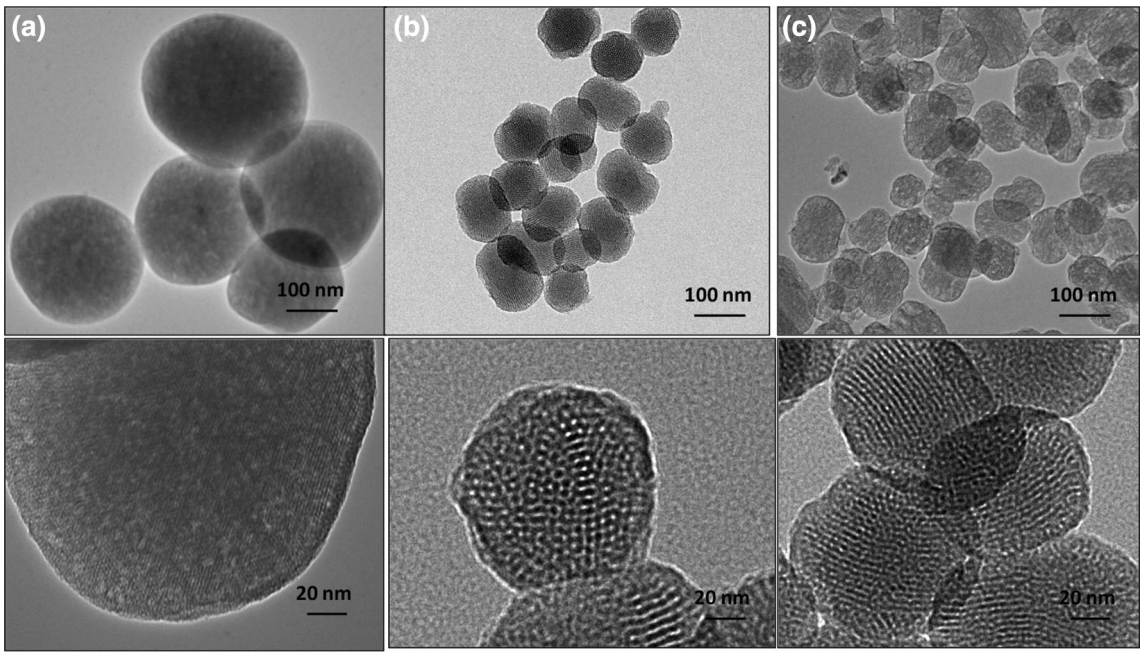


**Fig. 2** HRTEM micrographs of **a** MS-60, **b** MS-75 and **c** MS-90

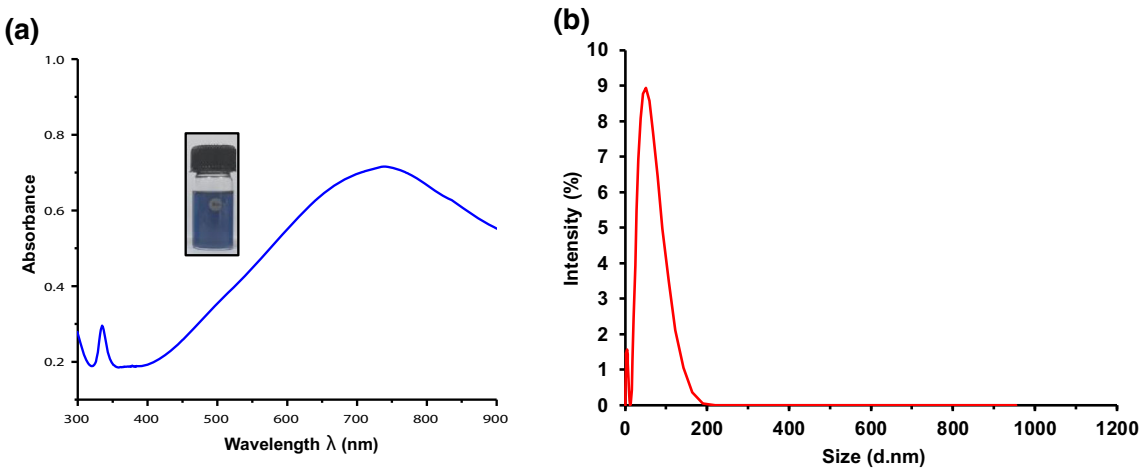


**Fig. 3** **a** UV–Vis spectra and **b** Particle size analysis of as synthesized Ag nanoparticles

have been investigated for plasmon-mediated photocatalysis (Chen et al. 2012). However, microporous $SiO_2$/blue Ag composite nanostructures have not been reported to the best of our knowledge. On account of better charge carrier generation, blue Ag NPs are likely to improve photocatalytic performance of $SiO_2$/blue Ag nanostructures in a significant manner.

In the present work, we have made an attempt to synthesis microporous silica/blue Ag composite nanostructures. The adsorption behavior of different dyes using microporous silica (MS) has been investigated. Amine-functionalized MS (MS-$NH_2$) was used for adsorption of blue silver nanoparticles on their surface. The synthesized MS-$NH_2$/Ag composite nanostructures were compared with MS-$NH_2$ nanoparticles for their photocatalytic behavior against methylene blue dye. MS-$NH_2$/Ag composite nanostructures are expected to have better adsorption of dye due to large surface area and porosity of microporous silica along with improved dye degradation facilitated by plasmon-assisted photocatalysis of Ag nanoparticles.

## Experimental

Microporous silica nanoparticles were synthesized using CTAB as a structure-directing agent and TEOS as precursor as reported by (Cao et al. 2016) with a slight modification. The obtained particles were coded as MS-60,

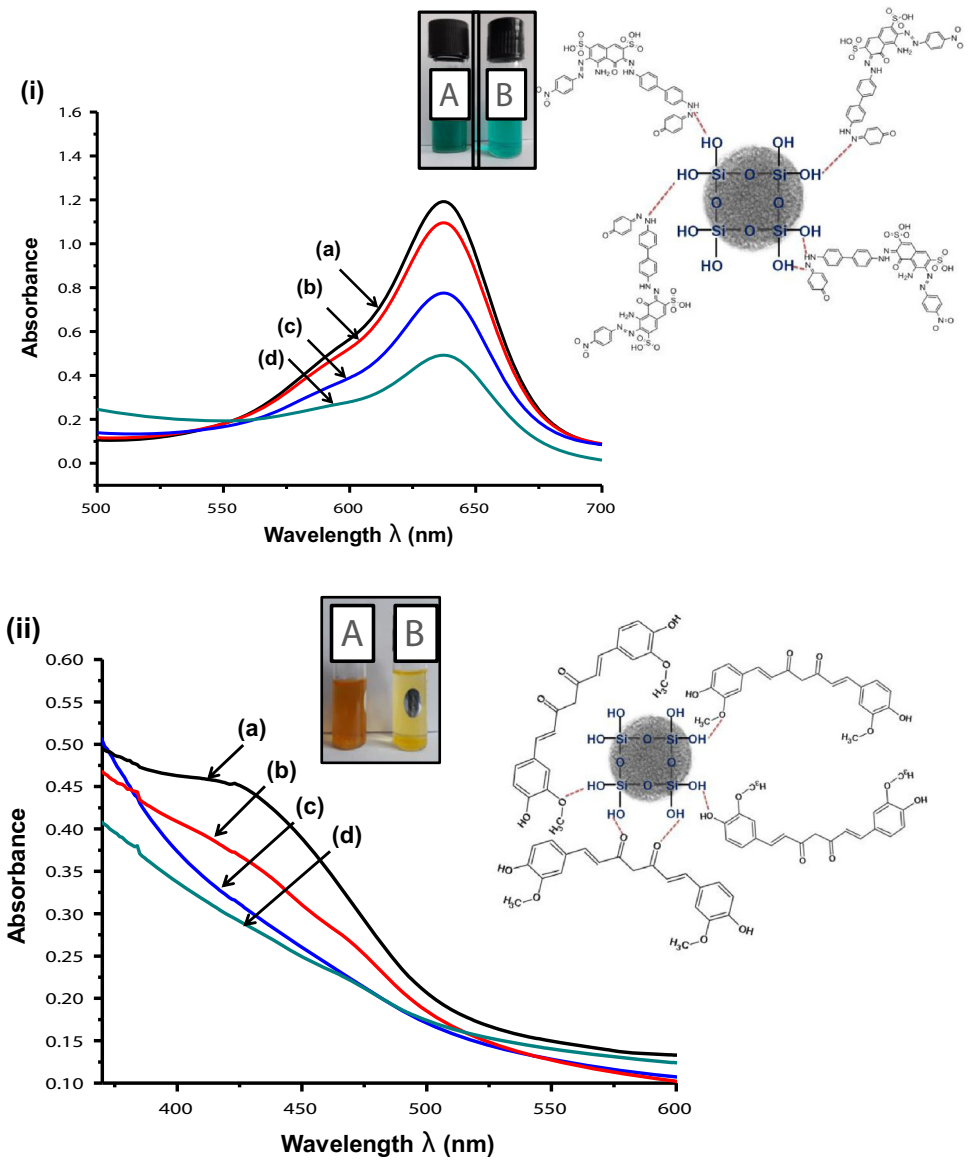


**Fig. 4** Adsorption of dyes with various functionalities **a** direct green 26, **b** curcumin crystalline, **c** methylene blue and **d** Congo red

MS-75 and MS-90 according to reaction time, i.e., 60, 75 and 90 min, respectively. The hydrolysis and condensation of the precursor, i.e., TEOS on the edges of the template followed by calcination, yielded porous morphology. The proposed mechanism of the synthesis is shown in Scheme 1. The obtained microporous silica nanoparticles were functionalized using APTMS ((3-aminopropyl) trimethoxysilane) and were coded as MS-60-$NH_2$. Curcumin crystalline, methylene blue, Congo red and direct green 26 dyes were used for adsorption analysis.

Silver nanoparticles were synthesized using $AgNO_3$ as precursor (Dong et al. 2010; Kelly et al. 2012) as mentioned in the supporting information. The obtained silver nanoparticles were characterized using a UV spectrophotometer (Lambda 35, PerkinElmer, USA), a particle size analyzer (Malvern Zetasizer Nano ZS, USA) and a high resolution transmission electron microscope (HRTEM). The blue Ag NPs were adsorbed on the surface of amine-functionalized microporous silica nanoparticles. Microporous $SiO_2$/blue Ag composite nanostructures were coded as MS-60-$NH_2$/Ag. Further, MS-60-$NH_2$ and MS-60-$NH_2$/Ag were compared for their photocatalysis behavior using 0.01 wt% methylene blue. Further experimental details of synthesis and characterization are provided in supporting information.

## Results and discussion

### Morphology of microporous $SiO_2$ nanoparticles

The morphology of the obtained $SiO_2$ nanoparticles was analyzed using a scanning electron microscope (SEM) and a high resolution transmission electron microscope

**Fig. 4** continued

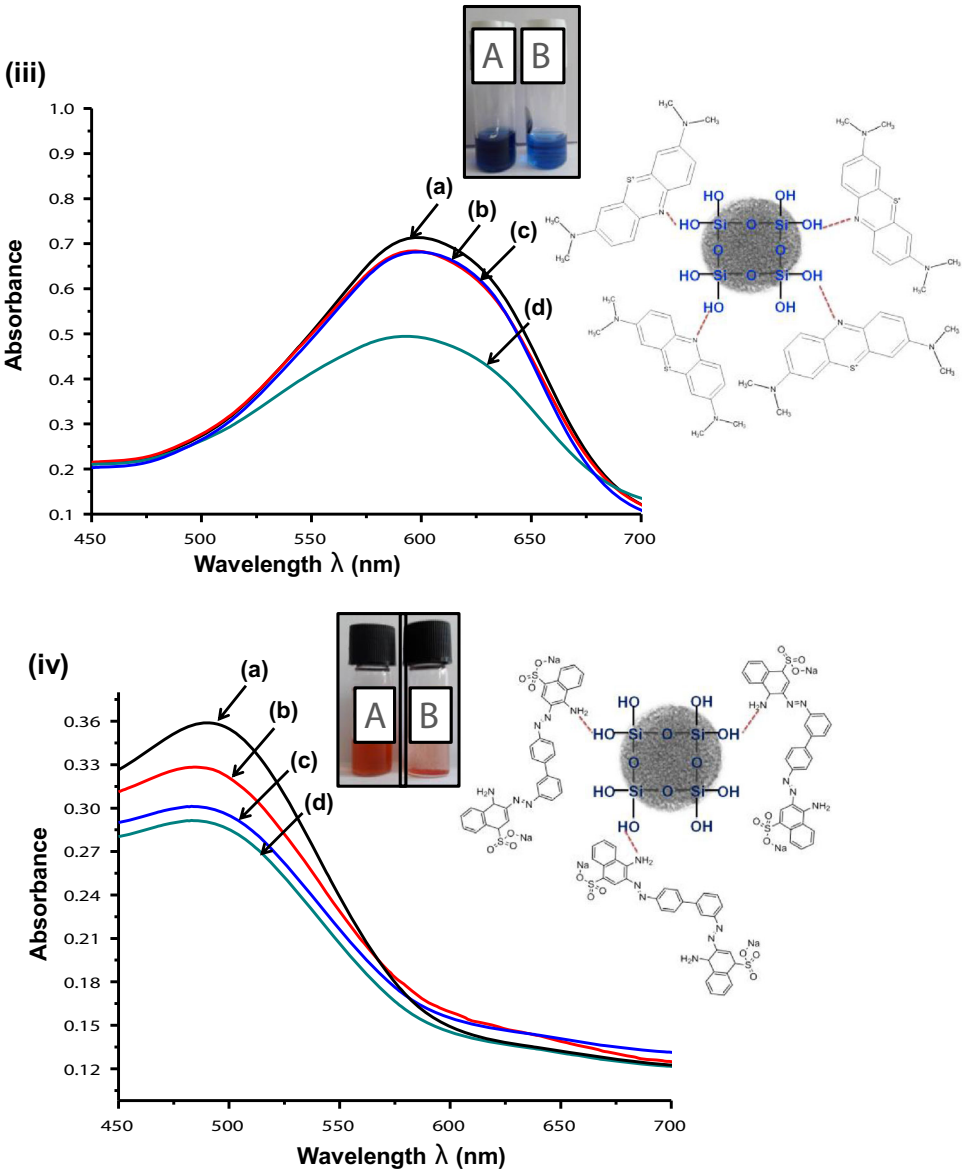


(HRTEM) as shown in Figs. 1 and 2, respectively. The histograms of particle diameter analyzed using SEM is shown in Figure S1. SEM analysis revealed that MS-60 nanoparticles were of spherical shape with an average diameter of 277 ± 74 nm. Further increase in reaction time to 75 and then to 90 min led to formation of more uniform and spherical particles with decreased diameter of 86 ± 12 and 72 ± 6 nm, respectively. It has been observed that the longer reaction time causes the reduction in diameter because of highly basic condition which results in etching of the particles (Chiang et al. 2011). The etching of particles makes them more uniform in diameter.

The porous nature of the silica was confirmed by HRTEM micrographs. The estimated pore size of the particles was found to be in the microporous range, i.e., 1.2 ± 0.5 nm.

## Characterization of silver nanoparticles

Particle size and UV–Vis spectroscopy analysis of triangular Ag NPs are shown in Fig. 3. UV–Vis spectra of the particles match with the literature, showing absorption maxima at 700 nm and peak corresponding to SPR at 329 nm. The triangular Ag NPs were found to have two peaks in particle size analysis, one at 3 nm and other at 50 nm (broad), respectively, indicating variation in particle diameter.

## Adsorption of dyes with various functionalities on the surface of microporous silica

The dyes with different functionalities including curcumin crystalline, methylene blue, Congo red and direct green 26

were used for adsorption studies. The 0.02, 0.2 and 1 wt% of MS-60 nanoparticles were analyzed for adsorption, and the decrease in dye concentration was estimated using a UV–Vis spectrophotometer as shown in Fig. 4. It has been observed that the concentration of dye was decreased on addition of MS-60 nanoparticles. The decrease in UV–Vis spectra corresponds to adsorption (not degradation) of dye molecules by MS-60. The decrease (%) was calculated using UV–Vis absorption spectra and was found to vary linearly with concentration of MS-60. Subsequently, the extent of decrease (%) of adsorption was measured and observed to be in the following order: direct green > curcumin crystalline > methylene blue > Congo red as shown in Fig. 5. The adsorption behavior of dyes was observed to vary according to their functional groups. It may be inferred from the results that high porosity and large surface area of microporous silica facilitate the adsorption of all studied dyes.

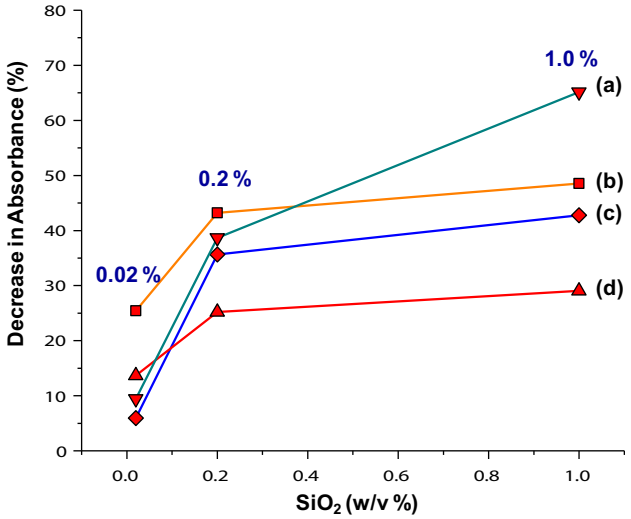


**Fig. 5** Adsorption of dyes with various functionalities **a** direct green 26, **b** curcumin crystalline, **c** methylene blue, **d** Congo red

Methylene blue is one of the most investigated dyes and therefore selected for photocatalysis. Fourier transform infrared spectroscopy (FTIR) analysis was carried out to investigate the interaction of methylene blue with microporous silica nanoparticles leading to its adsorption as shown in Fig. 6. The peaks at 800 and 3000–3700 $cm^{-1}$ corresponding to symmetric stretching of Si–O–Si and –OH, respectively, were found to be broadened. Further, the peak corresponding to –C=C stretching was found to be shifted from 1600 to 1635 $cm^{-1}$. The peak corresponding to asymmetric stretching of Si–O–Si at 1050–1150 $cm^{-1}$ disappeared indicating the interaction of dye molecules with the MS-60 nanoparticles (Lu 2013). This interaction resulted in adsorption of dye by microporous silica nanoparticles.

## Morphology of $SiO_2$/blue Ag composite nanostructures and their photocatalytic activity

$SiO_2$ offers large surface area due to its microporous nature and therefore acts as a good photocatalytic agent.

Adsorption of triangular Ag nanoparticles because of their enhanced SPR is likely to further improve photocatalytic behavior. To achieve better photocatalytic activity, $SiO_2$/Ag nanoparticles were synthesized by treatment of $SiO_2$ with APTMS followed by adsorption of blue silver nanoparticles on their surface as shown in Scheme 2.

The FTIR-analyzed spectra of amine-functionalized microporous silica nanoparticles are shown in Fig. 7. The stretching vibrations of hydrogen-bonded Si–OH and –OH

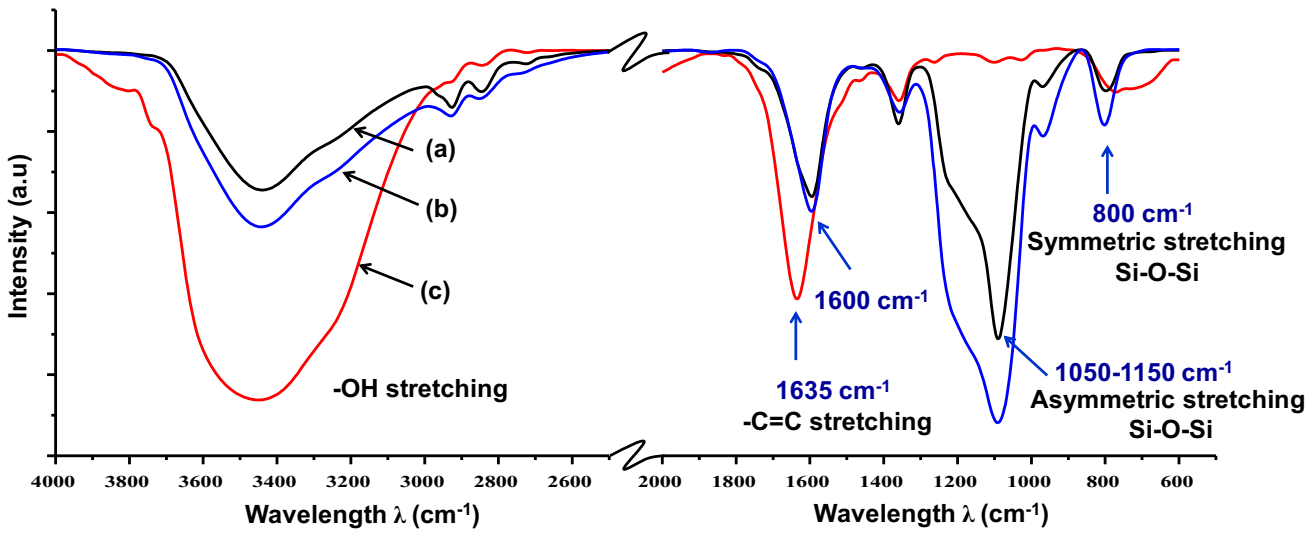


**Fig. 6** FTIR spectra of **a** MS-60 and **b** methylene blue dye and **c** dye adsorbed MS-60 nanoparticles

**Scheme 2** Functionalization of microporous silica nanoparticles and synthesis of $SiO_2$/Ag

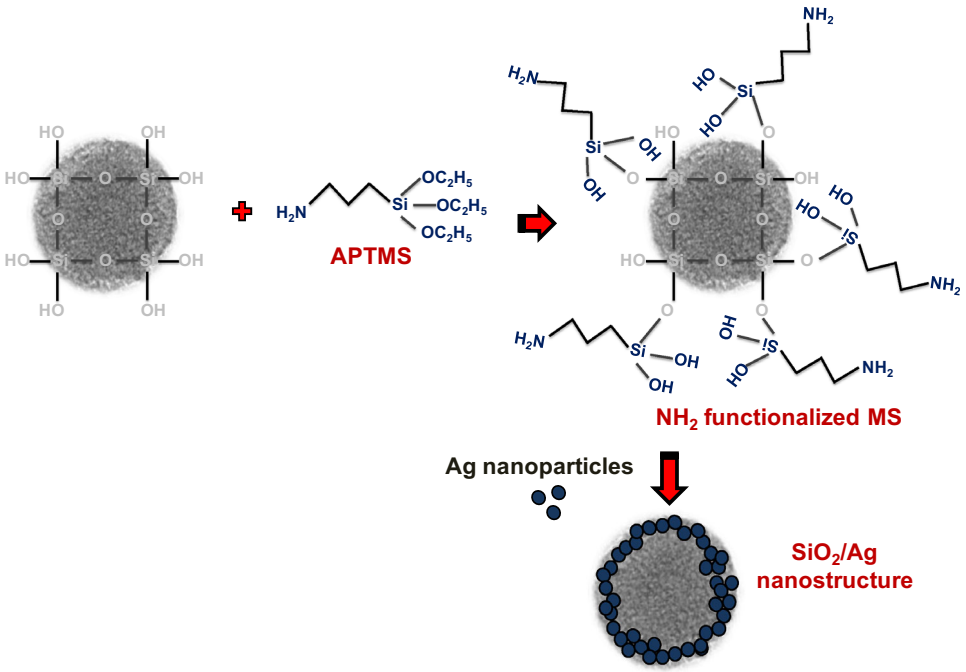


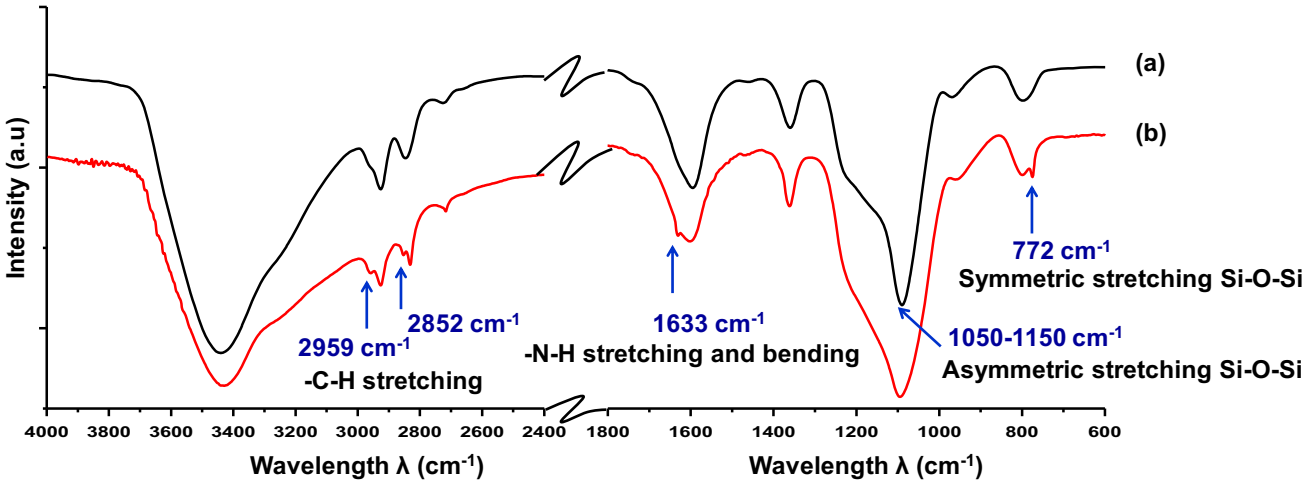


**Fig. 7** FTIR spectra of **a** MS-60 and **b** MS-60-$NH_2$ nanoparticles

**Fig. 8** HRTEM micrographs of **a** blue Ag nanoparticles, **b** MS-60-$NH_2$/Ag composite nanostructures

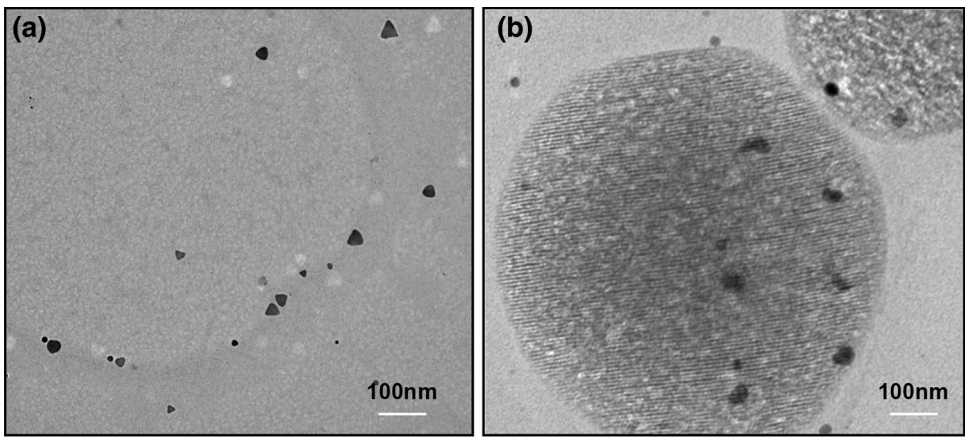

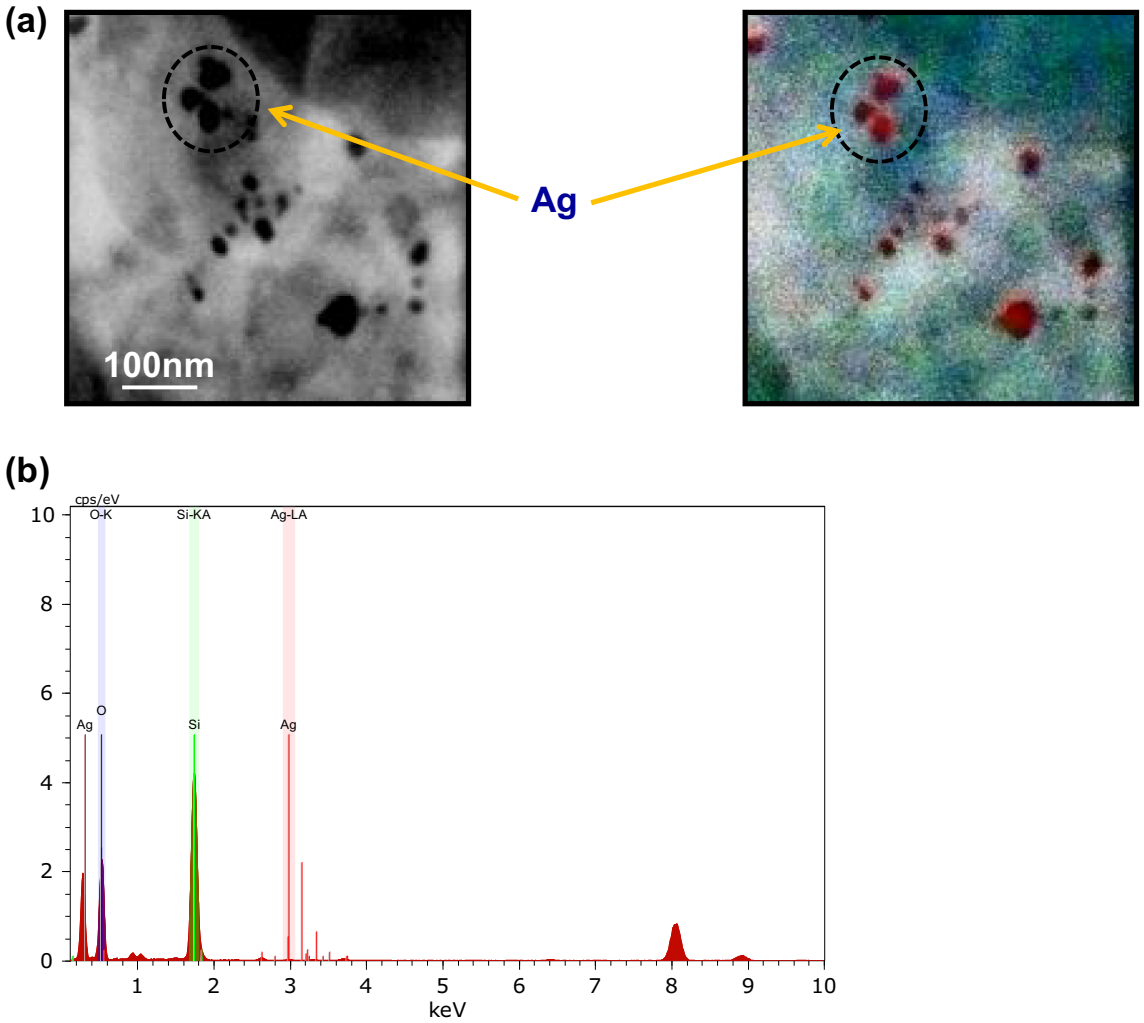


**Fig. 9** **a** HRTEM micrographs and **b** EDX spectrum of $SiO_2$/Ag composite nanostructures

of physically adsorbed water molecules and $–NH_2$ groups were integrated and as broad peak at 3425 $cm^{-1}$. The new peaks at 2959, 2852 and 1633 $cm^{-1}$ were attributed to asymmetric and symmetric C–H stretching of aminopropyl and $–NH_2$ bending vibrations, respectively (Castruita-de León et al. 2015). Splitting of Si–O–Si symmetric stretching peak at 772 $cm^{-1}$ further confirmed interaction of Si–O–Si with $–NH_2$ groups. These MS-60-$NH_2$ silica nanoparticles were used for adsorption of triangular silver nanoparticles.

The HRTEM analysis of triangular Ag NPs and MS-60-$NH_2$/Ag composite nanostructures is shown in Fig. 8. The micrographs revealed triangular shape of blue silver nanoparticles with an average size of 20 ± 10 nm. The adsorbed nanoparticles on the surface of mesoporous $SiO_2$ are clearly visible in the HRTEM micrograph and the presence of Ag was further confirmed by energy-dispersive X-ray (EDX) analysis (Fig. 9).

Thus, 0.2% (w/v) of MS-60-$NH_2$ microporous silica and MS-60-$NH_2$/Ag composite nanostructures were compared for their photocatalytic activity. The nanoparticles were dispersed in dye solution (0.01% w/v) followed by exposure to sunlight. The samples were placed in sunlight and visually observed for decoloration of dye and analyzed using UV–Vis spectrophotometer for photocatalytic behavior.

As shown in Fig. 10, the dye degradation was observed in both MS-60-$NH_2$ microporous silica and MS-60-$NH_2$/Ag nanostructures. However, the extent of decrease of the dye absorption was higher with MS-60-$NH_2$/Ag nanostructures (i.e., 97.3%) as compared to MS-60-$NH_2$ (i.e., 61.0%). The reduction in MS-60-$NH_2$ is due to adsorption of dye by microporous silica. Interestingly, the dye was found to decolorize within 1 min of exposure using MS-60-$NH_2$/Ag nanoparticles. Large surface area and porosity of microporous silica nanoparticles will make them good

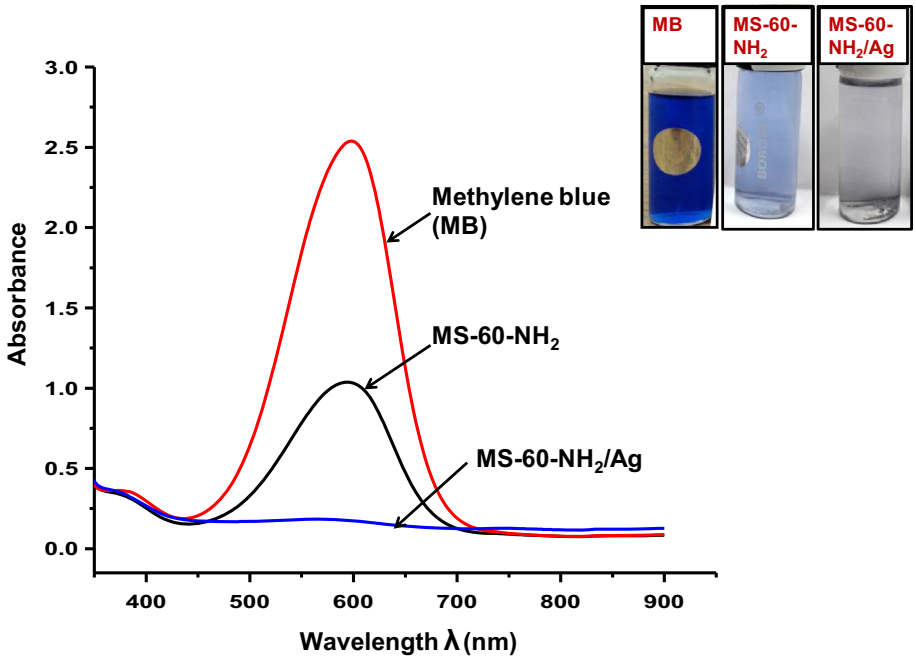


**Fig. 10** UV–Vis spectra showing degradation of methylene blue using MS-60-$NH_2$ and MS-60-$NH_2$/Ag

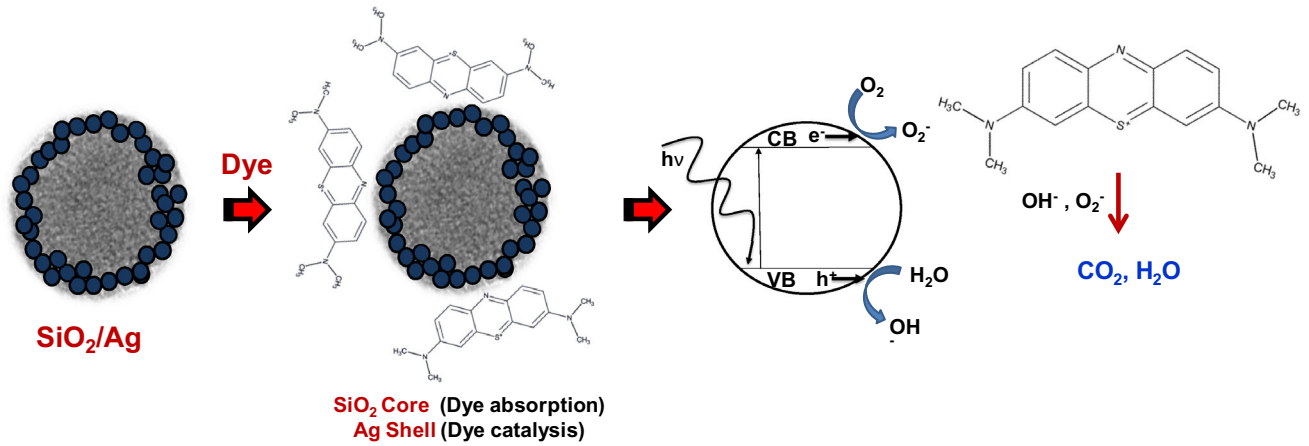


**Scheme 3** Photodegradation mechanism of methylene blue using MS-60-$NH_2$/Ag composite nanostructures

adsorbing material. The addition of Ag nanoparticles significantly improved the photocatalytic efficiency of MS-60-$NH_2$/Ag because of their plasmon-mediated photocatalysis. The expected mechanism of photodegradation is shown in Scheme 3. To quantitatively compare the photocatalytic performance of MS-60-$NH_2$ microporous silica and MS-60-$NH_2$/Ag nanostructures, the apparent rate constant for MB photodegradation ($k_{MB}$) was computed using the pseudo-first-order approximation. The $k_{MB}$ values of 0.94 and 4.2 $min^{-1}$ were obtained for MS-60-$NH_2$ and MS-60-$NH_2$/Ag nanostructures, respectively. The proposed MS-60-$NH_2$/Ag nanostructures offer applications in the area of waste water from textile industries.

## Conclusions

Microporous silica nanoparticles were successfully synthesized using CTAB as a structure-directing agent and varied reaction time. SEM and HRTEM analyses revealed that as the reaction time was increased from 60 to 75 and further to 90 min, the diameter was decreased from 277 ± 74 to 86 ± 12 nm and then to 72 ± 6 nm, respectively. HRTEM confirmed the microporous morphology of silica with pore size of 1.02 ± 0.5 nm. Adsorption of different dyes including curcumin crystalline, methylene blue, Congo red and direct green 26 was analyzed for 0.02, 0.2 and 1 wt% of MS-60 nanoparticles. Dyes exhibited

different extent of adsorption according to their functional groups in the order of direct green > curcumin crystalline > methylene blue > Congo red. Adsorption methylene blue dye, owing to its interaction with microporous silica nanoparticles, was confirmed using FTIR analysis. Synthesis of $SiO_2$/triangular Ag composite nanostructure was carried out by adsorbing synthesized blue Ag NPs on amine-functionalized microporous silica nanoparticles. The presence of Ag NPs on the surface of $SiO_2$ was evidenced by HRTEM and EDX analysis. Photon-mediated photocatalysis of $SiO_2$/Ag composite nanostructures was investigated and compared with pristine $SiO_2$ microporous nanoparticles. The UV–Vis spectra revealed a substantial improvement in degradation of methylene blue from 61% in $SiO_2$ microporous nanoparticles to 93% in $SiO_2$/Ag composite nanostructures, resulting in a colorless solution within 1 min of exposure. Large surface area and high porosity of microporous silica nanoparticles in combination with surface plasmon resonance of triangular Ag contributed to significant improvement in photocatalysis of $SiO_2$/Ag composite nanostructures.

**Acknowledgements** The authors would like to thank Bhaskaracharya College of Applied Sciences for providing the lab facilities and University of Delhi for financial support.

**Compliance with ethical standards**

**Conflict of interest** The authors declare no competing financial interest.



## References

Alimunnisa J, Ravichandran K, Meena KS (2017) Synthesis and characterization of Ag@$SiO_2$ core-shell nanoparticles for antibacterial and environmental applications. J Mol Liq 231:281–287. doi:10.1016/j.molliq.2017.01.103

Argyo C, Weiss V, Bräuchle C, Bein T (2013) Multifunctional mesoporous silica nanoparticles as a universal platform for drug delivery. Chem Mater 26:435–451

Aslan K, Wu M, Lakowicz JR, Geddes CD (2007) Metal enhanced fluorescence solution-based sensing platform 2: fluorescent core-shell Ag@ $SiO_2$ nanoballs. J fluoresc 17:127–131

Badr Y, Mahmoud M (2007) Photocatalytic degradation of methyl orange by gold silver nano-core/silica nano-shell. J Phys Chem Solids 68:413–419

Bandekar G, Rajurkar N, Mulla I, Mulik U, Amalnerkar D, Adhyapak P (2013) Synthesis, characterization and photocatalytic activity of PVP stabilized ZnO and modified ZnO nanostructures Applied. Nanoscience 4:199

Bharti C, Nagaich U, Pal AK, Gulati N (2015) Mesoporous silica nanoparticles in target drug delivery system: a review. Intern J Pharm Investig 5:124

Cao L, Zhang H, Cao C, Zhang J, Li F, Huang Q (2016) Quaternized chitosan-capped mesoporous silica nanoparticles as nanocarriers for controlled pesticide release. Nanomaterials 6:126

Castruita-de León G, Perera-Mercado YA, García-Cerda LA, Mercado-Silva JA, Meléndez-Ortiz HI, Olivares-Maldonado Y, Alvarez-Contreras L (2015) Synthesis of amino-functionalized MCM-48 silica via direct co-condensation at room temperature. Microporous Mesoporous Mater 204:156–162

Chen Y (2016) Synthesis of hollow mesoporous silica nanoparticles by silica-etching chemistry for biomedical applications. In: Design, synthesis, multifunctionalization and biomedical applications of multifunctional mesoporous silica-based drug delivery nanosystems. Springer theses. Springer, Berlin, Heidelberg, pp 31–46. doi:10.1007/978-3-662-48622-1_2

Chen X et al (2010) Supported silver nanoparticles as photocatalysts under ultraviolet and visible light irradiation. Green Chem 12:414–419

Chen K-H et al (2012) Ag-nanoparticle-decorated SiO2 nanospheres exhibiting remarkable plasmon-mediated photocatalytic properties. J Phys Chem C 116:19039–19045

Chiang Y-D, Lian H-Y, Leo S-Y, Wang S-G, Yamauchi Y, Wu KC-W (2011) Controlling particle size and structural properties of mesoporous silica nanoparticles using the Taguchi method. J Phys Chem C 115:13158–13165

Dong X, Ji X, Jing J, Li M, Li J, Yang W (2010) Synthesis of triangular silver nanoprisms by stepwise reduction of sodium borohydride and trisodium citrate. J Phys Chem C 114:2070–2074

Elmolla ES, Chaudhuri M (2010) Degradation of amoxicillin, ampicillin and cloxacillin antibiotics in aqueous solution by the UV/ZnO photocatalytic process. J Hazard Mater 173:445–449

Ghorai S, Sarkar A, Raoufi M, Panda AB, Schönherr H, Pal S (2014) Enhanced removal of methylene blue and methyl violet dyes from aqueous solution using a nanocomposite of hydrolyzed polyacrylamide grafted xanthan gum and incorporated nanosilica. ACS Appl Mater Interfaces 6:4766–4777

Giraldo L, López B, Pérez L, Urrego S, Sierra L, Mesa M (2007) Mesoporous silica applications. In: Macromolecular symposia, vol 258. Wiley Online Library, London, pp 129–141

Huang C-H, Chang K-P, Ou H-D, Chiang Y-C, Wang C-F (2011) Adsorption of cationic dyes onto mesoporous silica. Microporous Mesoporous Mater 141:102–109

Huang X, Young NP, Townley HE (2014) Characterization and comparison of mesoporous silica particles for optimized drug delivery. Nanomater Nanotechnol 4:2

Kelly J, Keegan G, Brennan-Fournet M (2012) Triangular silver nanoparticles: their preparation, functionalisation and properties. Acta Phys Pol, A 122:337–345

Krysztafkiewicz A, Binkowski S, Jesionowski T (2002) Adsorption of dyes on a silica surface. Appl Surf Sci 199:31–39

Li S, Ma Z, Wang L, Liu J (2008) Influence of MnO 2 on the photocatalytic activity of P-25 TiO 2 in the degradation of methyl orange. Sci in China Series B: Chem 51:179–185

Lu H-T (2013) Synthesis and characterization of amino-functionalized silica nanoparticles. Colloid J 75:311–318

Lu F, Wu SH, Hung Y, Mou CY (2009) Size effect on cell uptake in well-suspended, uniform mesoporous silica nanoparticles. Small 5:1408–1413

Nimrodh Ananth A, Umapathy S, Sophia J, Mathavan T, Mangalaraj D (2011) On the optical and thermal properties of in situ/ex situ reduced Ag NP's/PVA composites and its role as a simple SPR-based protein sensor applied. Nanoscience 1:87–96

Schneider J, Matsuoka M, Takeuchi M, Zhang J, Horiuchi Y, Anpo M, Bahnemann DW (2014) Understanding TiO2 photocatalysis: mechanisms and materials. Chem Rev 114:9919–9986

Sharma UK, Kushwaha M, Tiwari H, Prakash A (2014) A review on mesoporous silica nanoparticles loaded salbutamol sulphate. World J Pharm Pharm Sci 3:251–271

Sharmiladevi S, Priya AS, Sujitha M (2016) Synthesis of mesoporous silica nanoparticles and drug loading for gram positive and gram negative bacteria International. J Pharm Pharm Sci 8:196–201

Tang L, Cheng J (2013) Nonporous silica nanoparticles for nanomedicine application. Nano today 8:290–312

Wang W, Li Z, Gu B, Zhang Z, Xu H (2009) Ag@ $SiO_2$ core–shell nanoparticles for probing spatial distribution of electromagnetic field enhancement via surface-enhanced Raman scattering. ACS Nano 3:3493–3496

Wei L, Hu N, Zhang Y (2010) Synthesis of polymer—mesoporous silica nanocomposites. Materials 3:4066–4079

Wu G, Koliadima A, Her Y-S, Matijević E (1997) Adsorption of dyes on nanosize modified silica particles. J Colloid Interface Sci 195:222–228

Zhang G et al (2015) Hydroxylated mesoporous nanosilica coated by polyethylenimine coupled with gadolinium and folic acid: a tumor-targeted T 1 magnetic resonance contrast agent and drug delivery system. ACS Appl Mater Interfaces 7:14192–14200

**Publisher's Note**